Influence of the boundary condition on the first ply failure and stress distribution on a multilayer composite pipe by the finite element method.

O A González-Estrada, Juan León Becerra, A. Pertuz

Influence of the boundary condition on the first ply failure and stress distribution on a multilayer composite pipe by the finite element method

O A González-Estrada [1*], J S León [2] and A Pertuz [3]

[1] GIC, Universidad Industrial de Santander, Bucaramanga, Colombia.
[3] Department of Industrial Engineering, Universita degli studi di Salerno, Salerno, Italy.
[2] GIEMA, Universidad Industrial de Santander, Bucaramanga, Colombia.

E-mail: agonzale@uis.edu.co

Abstract. In this work, we study the influence of the boundary conditions in the stress distribution and the first ply failure of a commercially available multilayer composite pipe using a finite element model. An ASTM D2290 standard test was performed to determine the ultimate tensile strength and burst pressure. Also, an ASTM D3039 tension test performed on a longitudinal strip of the pipe was used to evaluate the elastic constants. We compared the experimental results with the numerical model to validate the material parameters used in the approximation. Hoop and axial stresses were obtained for three different boundary conditions: open, fixed and closed ends. Different failure criteria were considered to evaluate the first ply failure, and a comparison of failure criteria and boundary conditions was made.

1. Introduction

During the last years, composite pipes have been successfully used in the Oil & Gas sector mostly because their mechanical properties are very attractive, especially their weight to resistance ratio and their resistance to corrosion [1]. Other features such as ease of installation, high durability, and ease of maintenance make them more desirable than steel pipes. Different studies on the mechanical properties and laboratory tests have been carried out for their mechanical characterization [2–4].

Xia et al. [5], based on anisotropic tridimensional elasticity, gave an exact solution for the stresses and strains of an internal pressure pipe. This formulation was applied to the case of closed-end pipes, however, it is extensible to open-end conditions. There is not an analytical procedure to determine the stress distribution on a fixed-end boundary condition. Lekhnistskii [6] defined relations for the problem of plane stress in a cylindrical shell. Later, Tsai [7] included the plane strain (axial force different from zero). The material resistance was evaluated by two methods: first ply failure and last ply failure. Kanter et al. [8] investigated an analytical tool for composite thermoplastic pipes with the objective of correlating the results with laboratory tests such as tension, compression, internal and external pressure.

Quintero Ortiz et al. [4] examined the effect of scratches on the surface of composite pipelines for the transportation of hydrocarbons by experimental means. Soden et al. [9] performed rupture tests with tubular samples of epoxy glass fibre laminates, with 60% resin and ± 55 ° winding angles. Strain-stress curves showed nonlinear behaviour. Ferry et al. [10] showed that pipes exhibit varying types of

damaged elastoplastic behaviour depending on stress ratio axial stress/hoop stress. The extent of damage and plastic phenomena are responsible for non-linearity on stress-strain curves. They showed by micrographic analysis that microcracking is the main damaging process.

Numerical methods have been widely used to characterize properties and evaluate structural integrity for standard and advanced materials [11–15]. Reutov [11] studied, using finite elements, the multilayer pipes stress distribution for Oil & Gas applications, obtaining the equivalent stresses for each layer, where it was determined that the middle reinforced layer presents the maximum stresses for operation pressures. Bai et al. [16] investigated a mathematical and numerical model to analyse the collapse of the reinforced thermoplastic pipes (RTP), the results using finite elements (FE) reflected a minimal error percentage with respect to the theoretical analysis. Yu et al. [17] performed numerical analysis studies on RTP with aramid fibre. The results related the buckling failure with the angles between the reinforcement layers. De Sousa et al. [18] obtained results of stresses for the composite pipe type Riser, containing metallic and thermoplastic layers, from theoretical and numerical models. Anping et al. [19] performed a finite element analysis (FEA) to determine the mechanical properties of two types of composite pipes reinforced with steel wires.

Onder et al. [20] subjected a glass fibre reinforced plastic (GRP) pipe to internal pressure under closed-end condition, and burst strength is evaluated by analytical, FEA and experimental techniques. The Tsai-Wu criterion, the maximum stress, and the maximum strain theories were used to compute the burst failure pressure of the composite layers in a simple form. The FE method does not give an accurate burst pressure because strength reduction is not considered, just the first ply failure. Vedvik et al. [21] conducted an analysis for thick walled composite pipes with an isotropic liner, special attention was given to the process of damage. The research accounted for damage in the composite layer and plastic yielding in the isotropic layer.

In this work, the effect of the boundary conditions on the hoop and axial stresses is investigated for a commercially available pipe of reinforced fibreglass (Fiberspar®). A first ply failure pressure is obtained for each boundary condition according to different failure criteria. In section 2, the elasticity model for the pipe is presented. In section 3, the failure criteria are shown, following with the description of the experiments and the numerical models in section 4. Results and discussion are presented in section 5 and, finally, section 6 shows the conclusions.

2. Elasticity model for composite pipes

Flexible composite pipes of filament winding technology have anisotropic behaviour due to the different angles of the reinforcing layers. The pipes are characterized by having a low bending stiffness compared to steel pipes. The Fiberspar® pipe consists of 3 main layers [22]: PE 3408 high-density polyethylene (HDPE), inner and outer layer, and a middle layer with an Epoxy E glass fibre reinforcement.

Carroll et al. [23] conducted an experimental study of fibreglass with epoxy tubes with ± 55º winding angles with an internal diameter of 2 in. In [23] a test machine was used which allows different radial and longitudinal load ratios. The resulting stress-strain curves showed a complex behaviour of the tubes. The behaviour in the fibreglass pipes is elastic-linear at the beginning, followed by a non-linear behaviour near the fault, first by small leaks and second by ruptures. Generally, the nonlinear response is due to the formation of cracks in the matrix [24].

Consider the stress vector $\boldsymbol{\sigma} = \{\sigma_{xx}, \sigma_{yy}, \sigma_{xy}\}^{\boldsymbol{T}}$, displacements $\mathbf{u}$ and strains $\boldsymbol{\varepsilon}$, defined on the domain $\Omega \subset \mathbb{R}^{\mathbf{2}}$. Let us take $\mathbf{b}$ as the volumetric loads, $\mathbf{t}$ the Neumann tractions and $\bar{\mathbf{u}}$ the Dirichlet conditions. To solve the elasticity problem, we use a FE discretization such that we find the solution $\mathbf{u}^{\mathrm{h}} \in \mathbf{V}^{\mathrm{h}}: \mathbf{u} = \bar{\mathbf{u}}$ in $\Gamma_{\mathrm{D}}, \forall \mathbf{v} \in \mathbf{V}^{\mathrm{h}}$:

$$\int_{\Omega} \boldsymbol{\varepsilon}(\mathbf{v})^{\mathrm{T}} \mathbf{D} \boldsymbol{\varepsilon}(\mathbf{u}^{\mathrm{h}}) \mathrm{d}\Omega = \int_{\Omega} \mathbf{v}^{\mathrm{T}} \mathbf{b} \, \mathrm{d}\Omega + \int_{\Gamma_{\mathrm{N}}} \mathbf{v}^{\mathrm{T}} \mathbf{t} \; \mathrm{d}\Gamma. \tag{1}$$

The constitutive law $\boldsymbol{\sigma} = \mathbf{C}\boldsymbol{\varepsilon}(\mathbf{u})$ is expressed in terms of the stiffness matrix $\mathbf{C}$, defined by 9 independent constants for orthotropic materials. The constants $\mathbf{C}_{ij}$ are obtained from the classical

theory of laminates, considering the elastic properties of the fiber and matrix. The angular and longitudinal deformations are decoupled from the normal and tangential stresses. Furthermore, there is no interaction between the tangential stresses and the angular deformations in the different planes.

We consider a symmetrical laminate for the pipe, ensuring the continuity of the matrix in the direction orthogonal to the plane of the plies. The properties in the direction of the fibre differ from the properties in the direction of the main axes of the cylinder (axial, radial, and tangential). To identify the properties of the pipe it is necessary to know and establish the relationships with respect to the directions of the composite material. It is convenient to use two coordinate systems: one to define the local axes (1, 2) whose first direction coincides with the fibre direction, and another to define the global axes (*x, y, z*).

Given the geometrical characteristics of the ply, a plane stress state is assumed. The stress-strain relation for a unidirectional ply can be expressed as a function of the flexibility matrix $\mathbf{S} = \mathbf{C}^{-1}$ as:

$$\begin{Bmatrix} \varepsilon_1 \\ \varepsilon_2 \\ \gamma_{12} \end{Bmatrix} = \begin{bmatrix} S_{11} & S_{11} & 0 \\ S_{11} & S_{11} & 0 \\ 0 & 0 & S_{11} \end{bmatrix} \begin{Bmatrix} \sigma_1 \\ \sigma_2 \\ \tau_{12} \end{Bmatrix} = \begin{bmatrix} \frac{1}{E_1} & \frac{-\nu_{21}}{E_2} & 0 \\ \frac{-\nu_{12}}{E_1} & \frac{1}{E_2} & 0 \\ 0 & 0 & \frac{1}{G_{12}} \end{bmatrix} \begin{Bmatrix} \sigma_1 \\ \sigma_2 \\ \tau_{12} \end{Bmatrix}, \tag{2}$$

where the components of the flexibility and stiffness matrices have been replaced by the corresponding relations with the elastic constants of the ply E_1, E_2, G_{12}, ν_{12}, estimated from the properties of the constitutive materials. Each ply orientation uses a local coordinate system, and it is necessary to refer the individual response of each ply to the global coordinate system using a transformation matrix.

3. Failure criteria

Composite materials are not homogeneous, anisotropic and brittle, showing different failure modes, some related to the failure of the constituents and other to the interface [25].

In the fibres, two different failure modes can be considered: related to a tensile load and related to a compressive load. A characteristic of the fibre is that it does not usually show plastic deformation, the failure is related to a phenomenon of redistribution of stresses to the neighbouring fibres. This redistribution may cause a new fibre rupture. In the case of a compressive load, the progressive micro-buckling of the fibres takes place until the fibres break.

In the matrix, microcracking is the main mode of failure. This is equivalent to matrix cracks parallel to the fibre direction over the entire thickness of the ply and especially to those plies where the reinforcement is not in the same direction as the applied load.

Another common mode of failure is the disunion, which equals a loss of adhesion and a relative slip between the fibre and the matrix due to differences in shear stresses at the fibre-matrix interface [26].

For the design with composite materials, it is common practice to evaluate interactive failure criteria that take into account the interactions of the stresses.

3.1.1. Maximum stress and maximum strain criteria.

A ply fails if [27]:

$$\sigma_1 \geq X_1^T, \sigma_1 \geq -X_1^C, \sigma_2 \geq X_2^T, \sigma_2 \geq -X_1^C, \sigma_{12} \geq S, \sigma_{12} \geq -S \tag{3}$$

where X_i^T represents the uniaxial tensile strength of the ply in the *i* direction, X_i^C is the uniaxial compressive strength in the *i* direction, and S the shear strength in the plane. σ_1, σ_2 and σ_{12} represent the stress components in the 1-2 coordinate system.

The maximum strain criterion establishes that the ply fails if the strain is above a permissible strain. No interaction between different failure modes is permitted in these two approaches.

3.1.2. Tsai-Hill criterion.

This is a criterion based on the polynomial failure criterion and is one of the most used criteria, with results more adjusted to experimental values [25,28]. The Tsai-Hill criterion reads

$$\left(\frac{\sigma_1}{X_1^T}\right)^2 + \left(\frac{\sigma_2}{X_2^T}\right)^2 + \left(\frac{\sigma_{12}}{S}\right)^2 - \left(\frac{\sigma_1\sigma_2}{X_1^T}\right) \leq 1, \tag{4}$$

where the failure will occur for values greater than one. The disadvantage of Tsai-Hill is that it does not differentiate between strength to tension failure and compression during evaluation. In the case of compressive stresses, the compressive strengths are used in equation (4).

3.1.3. Tsai-Wu criterion.

Based on the Beltrami total energy deformation failure theory, for plane stress condition the failure is determined by the following expression [25,28]:

$$f_1\sigma_1 + f_2\sigma_2 + f_{11}\sigma_1^2 + f_{22}\sigma_2^2 + 2f_{12}\sigma_1\sigma_2 + f_{66}\sigma_{12}^2 \geq 1, \tag{5}$$

where $f_1, f_2, f_{11}, f_{22}, f_{66}$ are parameters described in terms of the ultimate strengths in the principal directions and f_{12} is determined experimentally with a biaxial stress test. Tsai-Wu is widely used in the analysis of progressive damage models for laminates since it allows to determine three-dimensional failure with a unique expression.

3.1.4. Hashin criterion

In [29], the authors indicated that it is not evident that all distinct failures modes could be expressed by a single function such as the foregoing criteria. They identified two mechanisms of failure: in the fibre and in the matrix, and provided expressions to identify each failure by considering separately traction and compression. For plane stress conditions the expressions read:

Fibre modes:

$$\left(\frac{\sigma_1}{X_1^T}\right)^2 + \left(\frac{\sigma_{12}}{S}\right)^2 = 1, \left(\frac{\sigma_1}{X_1^C}\right)^2 = 1. \tag{6}$$

Matrix modes:

$$\left(\frac{\sigma_2}{X_2^T}\right)^2 + \left(\frac{\sigma_{12}}{S}\right)^2 = 1, \left(\frac{\sigma_2}{2X_4}\right)^2 + \left[\left(\frac{X_2^C}{2X_4}\right)^2 - 1\right]\left(\frac{\sigma_2}{X_2^C}\right)^2 + \left(\frac{\sigma_{12}}{S}\right)^2 = 1, \tag{7}$$

where X_4 is the transverse failure shear.

3.1.5. Hoffman criterion

To consider the effects of isotropic stress in the Hill's equation for orthotropic materials, Hoffman included terms that are linear in the stress [30]. The failure criterion for plane stress reads:

$$-\frac{\sigma_1^2}{X_1^T X_1^C} + \frac{\sigma_1\sigma_2}{X_1^T X_1^C} - \frac{\sigma_2^2}{X_2^T X_2^C} + \frac{X_1^T + X_1^C}{X_1^T X_1^C}\sigma_1 + \frac{X_2^T + X_2^C}{X_2^T X_2^C}\sigma_2 + \frac{\sigma_{12}^2}{S^2} = 1. \tag{8}$$

4. Experiment setup and numerical model

The Fiberspar® pipes in their datasheet have a variety of operating conditions, ranging from 5.17MPa (750psi) to 17.23MPa (2,500psi), these pressures are known as nominal pressure or operating pressure. We selected a pipe with a nominal diameter of 50.8mm and operating pressure of 5.17MPa. Piping burst tests for this model have ranged from 27.17MPa (3,940.6psi) to 31MPa (4,800psi).

Two experimental procedures were performed. First, the apparent hoop tensile stress, ASTM D-2290, was done to obtain the ultimate stresses or burst pressure. Then, a tensile test, ASTM D3039, on a strip cut from a multilayer pipe was performed to obtain the elastic properties. Finally, a numerical model using the above parameters was developed on a complete pipe and under three different boundary conditions [10] to obtain the first ply failure and the stress distribution.

4.1. Apparent hoop tensile stress

In order to obtain the ultimate strength of the material, a tensile strength test was performed in the laboratory to obtain values of apparent normal stress under ASTM D-2290 [31], using a split ring segment with reduced section. The ASTM procedure for the proposed specimen, including the number of tests, data treatment, etc., is defined in [31]. The obtained average ultimate hoop stress is 81.44MPa, with a standard deviation of 7.81MPa [32].

To validate the numerical material model, we reproduce the ASTM experiment using finite elements for a half of the pipe by considering the conditions of symmetry. The apparent stress calculated on the minimum sample area corresponds to 82.31MPa, the error between the experimental test and the numerical model is 1.06%. These results help to validate the material model used in the numerical approximation for the commercial pipe.

4.2. Tension test

To obtain the values of the elastic constants, a tensile test was performed in an MTS Bionix uniaxial test machine [13], see **Figure 1**, following ASTM D3039 standard [33]. A finite element analysis of the strip was done, and the elastic properties were adjusted until a good agreement was found between the FE model and the experiment.

Figure 1. Tensile test on the MTS Bionix test machine for the composite pipe.

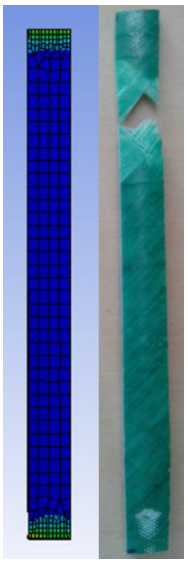

Figure 2. Experimental and numerical model of the longitudinal strip

The normal stresses show a homogenous distribution over almost all the length, however, near the traction surfaces the stresses are higher. This explains the zone of failure in **Figure 2**. To give an example, the displacement obtained with a 2,500N load by FE was 0.372mm and experimentally it was 0.353, just about a 5% error.

4.3. Numerical model

This section describes the finite element numerical approximation for a multilayer composite pipe subjected to internal pressure. It defines the geometry and material model, and the different boundary conditions used for the analysis of the stresses and first ply failure.

For the geometry, we reproduced the Fiberspar® pipe with an internal diameter 50.8mm. The internal diameter and external diameters for the different layers are: 59.79mm and 64.77mm for the external HDPE layer, 55.78mm and 59.79mm for the reinforced layer, and 50.8mm and 55.78mm for the internal HDPE layer. The reinforcement laminate is composed of 4 stacked plies with orientations of ± 55°, the configuration is [55/-55/55/-55]. Each ply has a thickness of 0.02in (0.502mm).

The mesh is made with order two hexahedral elements for the epoxy-fibreglass layer and for the inner and outer layers of polyethylene. Linear contact conditions were defined between the layers. The numerical model was implemented in Ansys v16.0. To control the discretization error, we made a mesh independence analysis set to 1% for the max. hoop stress, for a final mesh with 241,215 nodes.

The mechanical properties of the layers used in the model are shown in Table 1. The results for Young's modulus, Poisson's coefficients and shear stiffness moduli for the reinforcement layer correspond to the values calculated from the classical theory of laminates, and obtained experimentally. In the table, the subscripts 1 indicate the direction of the fibre, 2 the direction transverse to the fibre, and 3 the normal direction to the plane 12.

Table 1. Physical properties of the composite pipe layers.

Layer	Young´s Modulus			Poisson Ratio			Shear Modulus		
	E_1 (MPa)	E_2 (MPa)	E_3 (MPa)	ν_{12}	ν_{23}	ν_{13}	G_{12} (MPa)	G_{23} (MPa)	G_{13} (MPa)
Interior HDPE	1340	/	/	0,4	/	/	478,5	/	/
Epoxy-glass fiber laminate	35000	9000	9000	0,28	0,4	0,28	4700	3500	4700
Exterior HDPE	1340	/	/	0,4	/	/	478,5	/	/

Three boundary conditions were considered: (*i*) open-end condition, in which it does not exist axial stresses, this condition generally applies to pipes subjected to very elastic supports, (*ii*) fixed-end, in which the axial displacements in the ends are restricted in the normal direction, this is the case of very long pipes, and (*iii*) closed-end, condition known as pressure vessel condition [20]. An internal pressure of 5.17MPa (750psi) was applied in all cases.

5. Results and discussion

5.1. Stresses at nominal working pressure.

For the nominal working pressure of 5.17MPa (750psi), the main maximum stresses obtained are presented on the glass fibre reinforcement layer generating a maximum hoop stress of 61.4MPa, (the hoop stress distribution is the same regardless the boundary condition). The hoop stresses in the outer layer of HDPE were greater than those of the inner layer, see **Figure 3**.

The strain analysis shows that the layer with the greatest strain is the inner polyethylene with a deformation value along the ring of 0.018mm/mm and a minimum value in the outer layer of 0.01 mm/mm for a fixed-end condition. This condition holds true for the other two boundary conditions.

The results indicate that the ply of fibreglass composite closest to the inner layer presents greater stress and this decreases linearly towards the last layer. The stress is largely assumed by the laminate layer. The polyethylene layers work to protect the laminate layer from corrosion and transmit the greatest stresses to the composite laminate.

Figure 4 shows the distribution of the axial stresses across the dimensionless radius, it is observed that the open-end boundary condition sustains the smallest value of stress for any point across the thickness, fixed-end follows, and the closed-end is the highest.

5.2. First ply failure.

Using the different failure criteria, it is confirmed that for a working pressure of 5.17MPa there is no ply failure. The load was increased until the first ply failure is obtained, the results are shown in **Table 2**. In all cases, the first inner ply is the most critical, there may be fibre rupture or matrix microcracking rather than a complete failure of the pipe. The analysis performed for a pressure of 27MPa confirms that there is failure of all the plies.

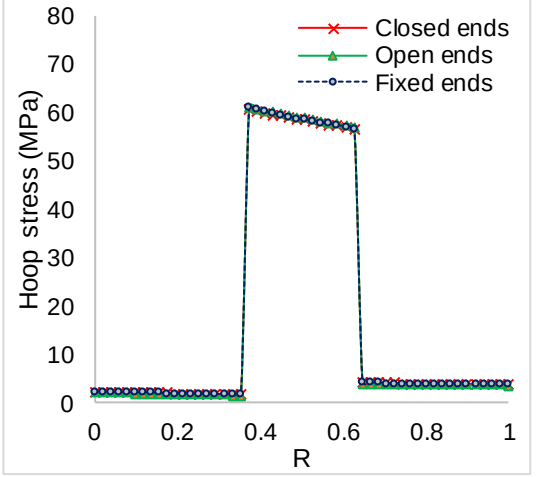

Figure 3. Hoop stress vs. the normalised radius R.

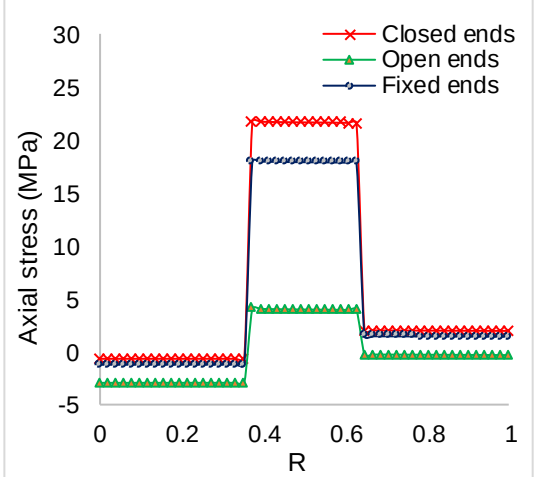

Figure 4. Axial stresses vs. the normalised radius R.

Table 2. FPF pressure for different failure criteria failure and boundary conditions.

Failure criteria	Open-end (MPa)	Fixed-end (MPa)	Closed-end (MPa)
Max stress	13.73	11.15	9.25
Max strain	16.13	14.97	9.96
Tsai-Hill	10.94	9.96	8.62
Tsai-Wu	10.87	10.70	9.41
Hoffman	10.48	10.06	8.82
Hashin	11.06	10.04	8.68

The maximum stress and maximum strain criteria show the highest values of FPF pressure, this is due to the fact that they do not take into account the stress interaction, the other criteria exhibit a lower FPF pressure and similar values between them. Regarding the boundary conditions, notice that the one that supports the highest pressure is the open-end condition, also called pure internal pressure.

The FPF pressure is near twice as double of the nominal pressure, and half of the final burst pressure, however, a burst pressure is not possible to obtain in this model because it does not take into account for a material degradation model.

6. Conclusions

The composite model for the Fiberspar® pipe was numerically defined. Particular interest was given to the definition of the fibre reinforced layer, and the model was validated through experimental tests. The error between the results of the laboratory test according to ASTM D2290 and the tensile numerical model is minimal. This validates the parameters used to define the computational model of the material.

Notice that when the orthotropic pipe is subjected to a pressure greater than 10MPa the first epoxy-fibreglass plies fails, but this does not mean that the pipe fails completely. At a burst pressure of 27.17MPa, the pipe fails on all the plies, and this point is called functional failure.

The values of the stresses on the pipe were determined for the three different boundary conditions, when it works at its nominal pressure of 5.17MPa. It was found that the composite laminate layer is the one that withstands the greatest stresses with a value of 62MPa for the hoop stress.

It was demonstrated that the FPF pressure for the open-end or pure internal pressure condition was the highest, this is because, in these conditions, the axial stresses are the lowest compared to the other ones. Additionally, the maximum strain and maximum stress criterion tend to over-estimate the FPF pressure because they do not consider the interaction between axial and hoop stresses.

Acknowledgements
The authors acknowledge the support given by the project Capital Semilla 1742, VIE, Universidad Industrial de Santander, and UIS-ICP Agreement 5222395, 'Structural integrity of spoolable composite pipes', 2016.

References

[1] Rafiee R and Amini A 2015 Modeling and experimental evaluation of functional failure pressures in glass fiber reinforced polyester pipes *Comput. Mater. Sci.* **96** 579–88
[2] Ji N, Geun H and Heum J 2013 Structural analysis and optimum design of GRP pipes based on properties of materials *Constr. Build. Mater.* **38** 316–26
[3] Hull D 1982 Research on composite materials at Liverpool University. I. Failure of filament wound tubes *Phys. Technol.* **13** 183
[4] Quintero Ortiz L A, Arciniegas Villamizar J R, Jiménez Romero M C, Vallen Vargas A Y, Amparo L, Ortiz Q, Ricardo J, Villamizar A and Vallen A Y 2015 Efecto en las propiedades mecánicas de daños superficiales generados en tubería compuesta flexible para transporte de hidrocarburos *Rev. Ing.* 39–48
[5] Xia M, Takayanagi H and Kemmochi K 2001 Analysis of multi-layered filament-wound composite pipes under internal pressure *Compos. Struct.* **53** 483–91
[6] S. Lekhnitskii 1963 *Theory of elasticity of an anisotropic elastic body* (San Francisco : Holden-Day)
[7] Tsai S W 1988 *Composite Design* (Dayton, OH: Think composites)
[8] de Kanter J L C G and Leijten J 2009 Thermoplastic Composite Pipe: Analysis and Testing of a Novel Pipe System for Oil & Gas *Proceedings of the 17th ICCM* (Edinburgh) pp 1–10
[9] Soden P D, Hinton M J and Kaddour A S 2004 Biaxial test results for strength and deformation of a range of E-glass and carbon fibre reinforced composite laminates. Failure exercise benchmark data *Fail. Criteria Fibre-Reinforced-Polymer Compos.* **62** 52–96
[10] Ferry L, Perreux D, Rousseau J and Richard F 1998 Interaction between plasticity and damage in the behaviour of [+φ, −φ]n fibre reinforced composite pipes in biaxial loading (internal pressure and tension) *Compos. Part B Eng.* **29** 715–23
[11] Reutov Y 2012 The calculation of multilayer polymer pipes using finite elements and their application to Gas and Oil pipelines *7th International Forum on Strategic Technology (IFOST)* pp 1–3
[12] Ayestarán A, Graciano C and González-Estrada O A 2017 Resistencia de vigas esbeltas de acero inoxidable bajo cargas concentradas mediante elementos finitos *Rev. UIS Ing.* **16** 61–70
[13] León B J S, González-Estrada O A and Pertuz A 2018 Damage in Fibreglass Composite Laminates Used for Pipes *Key Eng. Mater.* **774** 155–60
[14] Monserrat C, Tur M, Fuenmayor F, Nadal E, Rupérez M and Martínez-Sanchis S 2017 Evaluación basada en el método del gradiente de las propiedades elásticas de tejidos humanos in vivo *Rev. UIS Ing.* **16** 15–22
[15] González-Estrada O A, Pertuz A and Quiroga Mendez J E 2018 Evaluation of Tensile Properties and Damage of Continuous Fibre Reinforced 3D-Printed Parts *Key Eng. Mater.* **774** 161–6
[16] Bai Y, Tang J, Xu W, Cao Y and Wang R 2015 Collapse of reinforced thermoplastic pipe

(RTP) under combined external pressure and bending moment *Ocean Eng.* **94** 10–8
[17] Yu K, Morozov E V, Ashraf M A and Shankar K 2015 Analysis of flexural behaviour of reinforced thermoplastic pipes considering material nonlinearity *Compos. Struct.* **119** 385–93
[18] de Sousa J R M, Ellwanger G B and Lima E C P Modelo tridimensional de elementos finitos para el análisis de esfuerzos de tubos flexibles *Boletín Técnico* **42** 1–20
[19] Anping X, Peng S, Jingjing Z and Yunxia Q 2011 FEA-based Comparison of Two Kinds of Steel Wire Reinforced Composite Pipes *4th Int. Conf. Intell. Networks Intell. Syst.* 184–7
[20] Onder A, Sayman O, Dogan T and Tarakcioglu N 2009 Burst failure load of composite pressure vessels *Compos. Struct.* **89** 159–66
[21] Vedvik N P and Gustafson C G 2008 Analysis of thick walled composite pipes with metal liner subjected to simultaneous matrix cracking and plastic flow *Compos. Sci. Technol.* **68** 2705–16
[22] Quigley P A, Nolet S C and Williams J G 2000 Composite spoolable tube 2002
[23] Carroll M, Ellyin F, Kujawski D and Chiu A S 1995 The rate-dependent behaviour of ± 55 ° filament-wound glass-fibre/epoxy tubes under biaxial loading *Compos. Sci. Technol.* **55** 391–403
[24] Abdul Majid M S, Majid A, Bin M S and Abdul Majid M S 2012 *Behaviour of Composite Pipes Under Multi-Axial Stress* (Newcastle University)
[25] Molinier M 2006 *Análisis de los criterios de falla aplicados a los laminados compuestos* (Buenos Aires)
[26] Arias Maya L and Vanegas Useche L 2004 Falla de los materiales compuestos laminados *Sci. Tech.* 113–8
[27] Barbero E J 2013 *Finite Element Analysis of Composite Materials Using ANSYS* (Boca Raton, U.S.A.: CRC Press)
[28] Tuttle M E 2004 *Structural Analysis of Polymeric Composite Materials* ed M Dekker (New York, U.S.A.)
[29] Hashin Z 1980 Failure Criteria for Unidirectional Fibre Composites *J. Appl. Mech.* **47** 329–34
[30] Jones R M 1998 *Mechanics of composite materials* (Press, CRC)
[31] ASTM 2290-16 2016 Standard Test Method for Apparent Hoop Tensile Strength of Plastic or Reinforced Plastic Pipe *ASTM Int.*
[32] González-Estrada O A, Leal Enciso J and Reyes Herrera J D 2016 Análisis de integridad estructural de tuberías de material compuesto para el transporte de hidrocarburos por elementos finitos *Rev. UIS Ing.* **15** 105–16
[33] ASTM D3039/D3039M-14 2014 Standard Test Method for Tensile Properties of Polymer Matrix Composite Materials *ASTM Int.* 1–13